BREAKDOWN SPECTROSCOPY STIMULATE BY LASER FOR SILVER PLASMA

Naveen*

Open Researcher, Department of Physics
Jind, Haryana, India

***Email ID**: naveenmor7313@gmail.com*

Accepted: 08.11.2022 **Published**: 01.12.2022

Keywords: Nanomaterial, Low-Intensity Background Scattering (LIBS), Silver Langmuir.

Abstract

The optical absorption spectrum, or I'n, of gold (Ag) plasma were the primary topic of this paper. This was accomplished by the stimulated laser breakup spectroscopy procedure. In order to determine the exact link between light beam energies, measurements not only of the strengths of emission lines but also plasma properties were carried out. Both the electron density, which is denoted by the symbol ne, and the temperature, which is denoted by the symbol Hou, have been computed using either classic Blotzmann polt method or the McWhirter criteria. At the essential wavelengths (1064 nm), the data points of (ne) but also (Te) have a band of (6064 through 4507K), where (ne) equals (2.3x1017 through 3.7x1017 mm), while the case pf (Ag- ba), the figure of electron density became The quantity of electrons packed into a certain space (9.36x1016 to 1.19x1017cm-3). Overall temperature of both the electron, denoted by Te, was shown to rise suddenly as a direct consequence of an increase inside the light beam energy. This was a prevalent tendency among the studies. because the density of the electrons rises in proportion to the increase throughout energy.

Paper Identification

**Corresponding Author*

I. Introduction

(Since its discovery in the 1960s, the Laser Induced Degradation Spectroscopy (often abbreviated as LIBS) technique has garnered the attention of researchers spanning many generations. This kind of delicate technique relies on (optical revelation) with respect to a wide variety of molecules and atoms types in order to acquire subsequent emission from laser-motivated gas. The control of the chemistry and physical features of a wide variety of materials, including liquids, minerals, minerals, polymers, aerosols, biological products, and.....etc., may unquestionably benefit from the use of this technique, since it is widely regarded as an effective method .

As a result of the uncomplicated nature of such experimental setting, the process does not present any challenges and may be compared to many kinds of elemental research. During the step that came before,

we needed the assistance of a pulsed device to generate micro plasma upon that material's surface. By having prior knowledge of the ionization plume emission, this elemental analysis may be done with more competence. The stimulate foam or, in these other words, the induced gas by optical is influenced by a variety of distinct factors that determine the advantages of desired target, characteristic of surroundings, laser's wavelength, period of burst, and so forth and so forth forth. The first work on the spectrum analysis was done with (LIBS), which may be connected with. There in 1980s, this method became more popular for use in scientific research as both a clinical instrument . Because of its great conductivity, it is being studied in conjunction with other metals for a wide variety of applications as plasmonic nanomaterials .

The characteristics of dispersion as well as the characteristics for corona of silver are particularly significant in laboratory plasma diagnosis or for various technological applications, such as the manufacture of clusters, the interconnection of low-voltage instruments, nanoparticles, and metals films.

II. Experimental Work

The set-up of the experiment that applied for the measure of silver plasma is clarified as:

The laser Nd: YAG working at 1064 wavelengths . The pulses with the maximum energy is directed towards the cause of the burn and is administered (850mJ). The self - renewal of the lasers could be altered by the use of the beam's control, and this was accomplished by use of a power meter (Pro Quantel 0.001) by delaying the flash light's Q-switch.

The optical device instrument consists of a converging lens with just a telephoto lens of ten centimeters as well as mirrors made from brass and designed for plane reflection. These mirrors have a width of fifty millimeters and a width of ten millimeters (5mm). The spectral emission that was noticed by making use of a vigorous tempo of radiation that had been recorded during the same circumstances. The (photonic fiber) that originates from ocean optics was used in order to collect the plasma electromagnetic waves.

Co (core diameter: 600 microns, elevated) have just a beam splitter lens that is situated in the correct angle which accompanies laser radiation. its field of vision ranges from 0 to 45 degrees. The HR 5000 spectrometer has been linked to the fiber optics inside that contains of 14 diffraction which is accessible m), which lid'to entry cut (5, 10, 25, 100, plus 200 the region from (200-1100micrometers) of spectral with just a sharpness of optical approximately (0.03nm), and also the duration for integration is about (3.8ms-10sec).

The object was targeted using ocean optical on even a 3D experiment stage, which had been moved to avoid the target caused by irregular pitting. The platinum target was formed in the format of a rectangle and also was 4 centimeters across with only a height of 3.0 millimeters.

III. Result and Discussion

The Spectrum of Optical Emission for Silver Bulk

The laser Nd: Rest and relaxation was set at 1064 nanometers, and the length of the pulse were 6 nanoseconds, while the repetition rate being 10 hertz. This created a plasma comprising silver. The strength of the light that was specified to the substratum for the Mag target was recorded as having been emitted by the plasma.

(140 versus 225 mJ) were noted at the agribusiness substrate for such emitters of serum the with direction of spread at the requisite environment, and indeed the consequence of Ag emitters was within a spectrum of

(approximately 100 to visible range) first from wavelength range such as the Plum. (2-3 but instead 4), that either clearly demonstrates that the astral regions recieved well separated, that as Asst emission resultant both by unbiased atoms or particles of Ag.

Ag (I) is associated with the (200-595 nm) of something like the spectrum area between is associated with Ag (I); however, on the contrary hand, the (260-404 nm) range appears attendance both A (I) plus Ag (II), and then for (360-520 nm), there also emerged neutral cationic Ag atoms with the mingled streaks. 546.55, 786.77, but also 827.35 wavelengths) were used to generate the signals of the spectra lines around, and indeed the NBS (Ins) database server was utilized in order to make the identification.

Because of the surprised wave's competitors at the objective of the Metal substrate, the created plasma had a relatively limited duration and a drawn-out course. The setup states that are overwritten by parallel transitions are shown in (Table1) together with their respective transition probabilities.

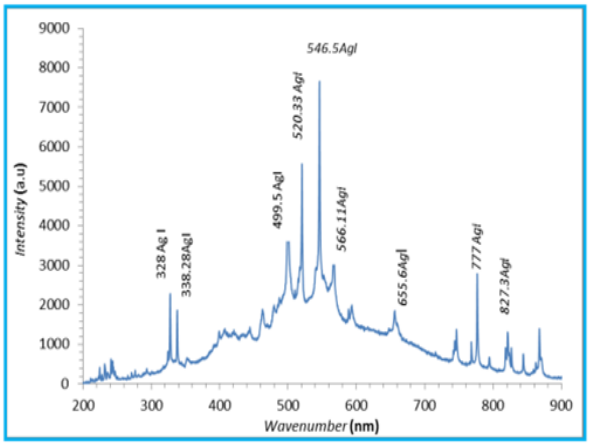

Figure 1. Emission profile of neutral versus ionized silvery plasma, created by a photons lamp at such a 5 millimeter distance mm, with 140 mJ total laser energy, encompassing the area with a spectral range of 200-900 wavelengths.

This band was a decent determination that exhibits doublet organization from an assortment of layers which were stimulated and degraded to reduced ranks. This gives it more significance and makes it more useful spectroscopically about plasma temperatures and the amount of electrons in the liquid. The transformation from 4d9 5p3F3 into 4d95s 3 D2 but also 4d95p3P2 into 4d95s 3D3 Mag (II) with the least wavelength property compared to the earlier formulation.

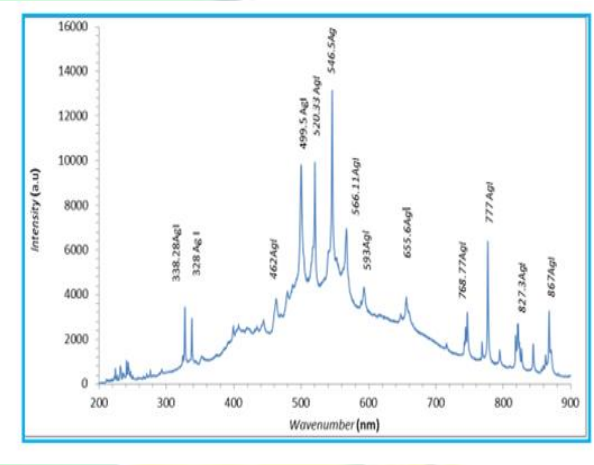

Figure 2. The emitted spectrum of free and ionized silvery plasma, created by such a 1064 nm light at a wavelength of 5 mm with 225 mJ pf laser pulses, encompassing the range of 200-900 wavelengths in the broad window

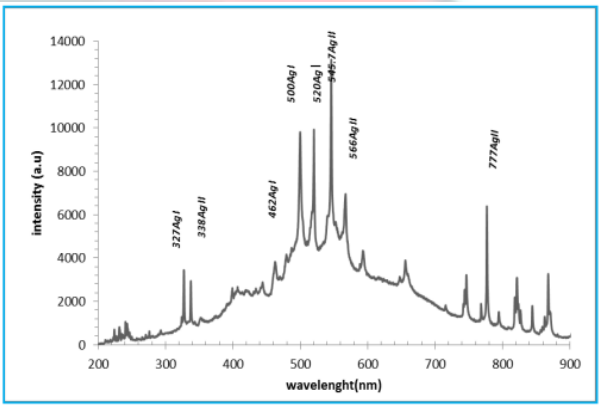

Figure 3. Emission pattern of neutral versus ionized silvery plasma created by a 1064 nm light at such a

wavelength of about five mm, with a laser pulses of 200 michael jackson, encompassing the area with a spectral windows of 200-900 wavelengths.

The Plasma Temperature

The Bayesian plot method was used to compute the temperatures of the sensor silver plasma. This method requires that the anticipated plasma that satisfies the LTE scenario be thin visually. Additionally, the number concentrations in the active state follow standard Boltzmann allocation. Under these conditions, the velocity of the electrons that has been calculated via the line and argent for the identical state of quantization as (Howard, 2002) is shown in equation outlined in the following:

$$\frac{hc}{4\pi}\frac{Aijgi}{\lambda ijU(T)}ne^{-Ei/KT}\frac{hc}{4\pi}\frac{Aijgi}{\lambda ijU(T)}ne^{-Ei/KT}$$

The inevitable of handrail is denoted by the letter h, the inevitable of Thermodynamics is denoted by the letter k, the velocity of light has been denoted by the letter c, the thermostat of the bloodstream is denoted by the letter T, and indeed the component of separation is denoted by the letter U (T). Yet another, the possibility of transformation is denoted by the letter Aij, while glycemic index represents the depravity of the top floors and Ei . by the process of taking this same log transformation of the value and reorganizing it. (2),

$$\ln\left(\frac{I_{IJ}\lambda}{g_{I,Z}A_{IJ}}\right) = -\frac{Ei}{K_B T} + \ln\left(\frac{hcn_T}{4\pi U_T}\right)$$

temperature estimate. Table 1 included both the detection approach as well as the spectrum lines that were seen. The plot generates a line that looks like straight ahead, and the temperatures of the plasma can be pulled from the slope of -1/kTe.

Plasma was produced by varying the laser resources and energy among both 125 but also 200 mJ. This same Boltzmann plot figures (5, 6, but also 7) were used to decide the Te. During the laser heartbeat exposure period, an area adjacent to the exterior of the particular compound regularly soaked up the luminance, which is responsible around charged particle permits for air temp obtaining and based on Boltzmann narrative figs (5, 6, but also 7), the plasma material is heated among both 6564, 5228, but also 4507 kelvin.

Around the surface, another temperature rise is caused by inverse bremsstrahlung pumping, which occurs when laser eradiation gets absorbed. However, a reduction in temperature occurs when thermal energy is swiftly transformed into angular momentum.

Table 1. Spectroscopic data of Ag lines used for temperature calculation [11]

Wavelength (nm)	Transitions	Statistical weight	Transition probability A(s^{-1})		Upper level Energy Ek(cm^{-1})
gi			gk		
328.068	4d10 5p 2P3/2----- $4d^{10}$ 5s 2S1/2	2	4	1.4 x 108	30472.703
338.289	4d105p 2P1/2---4 d^{10}5s 2S1/2	2	2	1.3 x 108	29552.061
520.907	4 d105d 2D3/2--4d^{10}5p 2P1/2	2	4	7.5 x 107	48743.969
546.550	4d105d 2D5/2--4d105p 2P3/2	4	6	8.6 x 107	48764.219
768.77	4d106s 2S1/2--4d105p 2P1/2	2	2		42556.152
827.351	4d106s 2S1/2-- 4d105p 2P3/2	4	2		42556.152

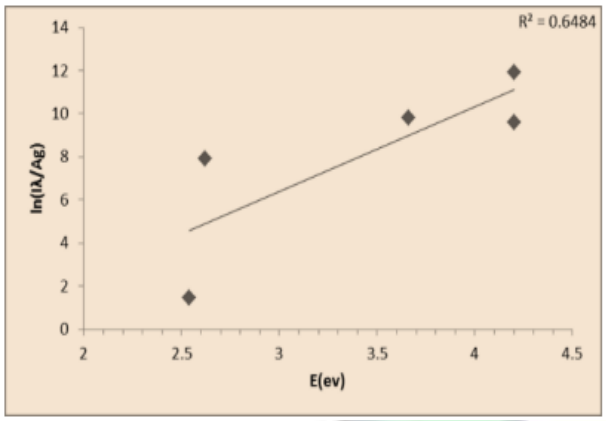

Figure 4. Boltzmann plot for (5) neutral spectral lines produced by the 1064 nm Nd:YAG laser irradiation with 140mJ

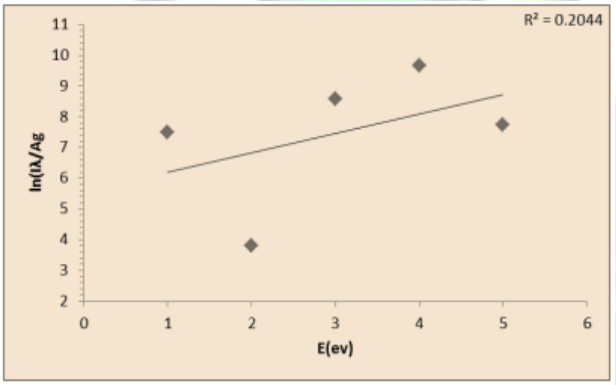

Figure 5. Boltzmann plot for (5) neutral spectral lines produced by the 1064 nm Nd:YAG laser irradiation with 200mJ

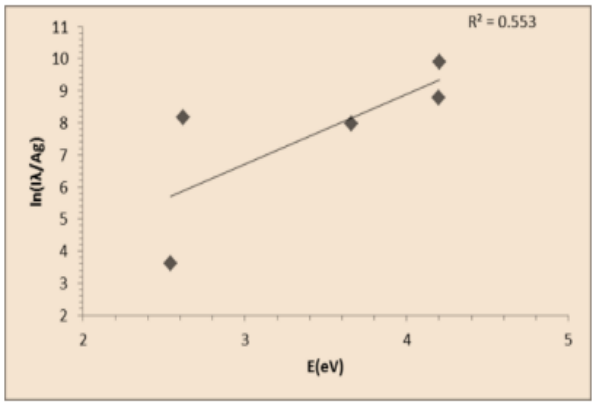

Figure 6. Boltzmann plot for (5) neutral spectral line produced by the 1064 nm Nd:YAG laser irradiation with 225mJ

The Electron Density Number

As a result of the fact that the nuclear and polyatomic states ought to be staffed and depopulated predominately by electron accidents, rather than through radiation, there is a requirement for an electronic structure that is adequate to guarantee a high risk of a crash. This is because of the situation described above. In accordance with the McWhirter criteria (McWhirter, 1965), the following is the corresponding cutoff point of the charge distribution:

$$Ne \geq 1.6\times10^{12}T^{1/2}\Delta E_3$$

When T (K) is indeed the temperature of the ionized and E (band gap energy) is really the basic difference seen between states that are anticipated to be located in local equilibria (LTE) around 11600k temperature, then equation (3) results in ne less than 1015 cm-3. Under these circumstances, the collision was responsible for the majority of the radiation emission in the plume. The number of electrons per unit volume that was computed for various laser intensities.

As shown in the results of Table 2, take notice that the number of electrons in the density varies among (9.36x1016 to 1.19x1017cm-3). This was discovered that the quantity of electrons in the cherry was rising when the laser powers were increased. This occurred as a result of the plums absorbing and reflecting laser photons. As the expunction flounce is increased, a greater number of species, ions, and electrons are produced, and the femtosecond pulsed reacts with these species.

Table 2. The Plasma temperature and electron density number at different laser energy

Laser pulse energy (mJ)	T_e (k)	N_e cm^{-3}
200	6064	$9.36x10^{16}$
225	5228	$1.19x10^{17}$
140	4507	$1.0x10^{17}$

IV. Conclusion

This study primarily focused on doing a comprehensive examination of nanosecond precision plasma of core Ag. For the purpose of collecting temporary ionization spectra inside the spectral region of (200-900) wavelengths, the technique of spectral disclosures is being used. We conducted an investigation of the particles temperature as well as its electronic structure to use a model of local equilibrium conditions. The findings indicate that now the plasma characteristic Ag bulk.

REFERENCES

- Anabitarte F, Cobo A, Lopez-Higuera JM. Laser-induced breakdown spectroscopy: fundamentals, applications, and challenges. International Scholarly Research Notices 2012.
- Brennetot R, Lacour J, Vors E, Fichet P, Vailhen D, Maurice S, Rivoallan A. Trends in Optics and Photonics. Laser induced plasma Spectroscopy and Applications, OSA Technical Digest 2002: 81.
- Cremers D, Radziemski L. Handbook of Laser-Induced Breakdown Spectroscopy. John Wiley & Sons. Haboken 2006.
- Cristoforetti G, De Giacomo A, Dell'Aglio M, Legnaioli S, Tognoni E, Palleschi V, Omenetto N. Local thermodynamic equilibrium in laser-induced breakdown spectroscopy: beyond the McWhirter criterion. Spectrochimica Acta Part B: Atomic Spectroscopy 2010; 65(1): 86-95.
- Howard J. Introduction to plasma physics. Plasma research laboratory, Research school of physical sciences and engineering, Australian national university 2002.
- Li M, Bo X, Mu Z, Zhang Y, Guo L. Electrodeposition of nickel oxide and platinum nanoparticles on electrochemically reduced graphene oxide film as a nonenzymatic glucose sensor. Sensors and Actuators B: Chemical 2014; 192: 261-268.
- McWhirter RWP. Plasma Diagnostic Techniques. Edited by Richard H. Huddlestone and Stanley L. Leonard. Library of Congress Catalog Card Number 65-22763 1965.
- Miziolek AW, Palleschi V, Schechter I.(Eds.). Laser induced breakdown spectroscopy. Cambridge university press 2006.
- Musadiq M, Amin N, Jamil Y, Iqbal M, Naeem MA, Shahzad HA. Measurement of electron number density and electron temperature of laser-induced silver plasma. International Journal of Engineering & Technology 2013; 2(1): 32-43.
- NIST Atomic Spectra Database, "Kurucz Output Atomic Spectra Line Database from R.L.KURUCZ atomic spectral line database. http://www.pmp.unihannover.de/cgibin/ssi/test/kurucz/ sekur/sekur.html
- Noll R. Laser-induced breakdown spectroscopy. In Laser-Induced Breakdown Spectroscopy, Springer, Berlin, Heidelberg, 2012: 7-15.
- Rashid B, Hafeez S, Shaikh NM, Saleem M, Ali R, Baig MA. Diagnostics of copper plasma produced by the fundamental, second and third harmonics of a Nd: YAG laser. International Journal of Modern Physics B 2007; 21(15): 2697-2710.
- Runge EF, Minck RW, Bryan FR. Spectrochemical analysis using a pulsed laser source. Spectrochimica acta 1964; 20(4): 733-736.

- Sanghavi BJ, Wolfbeis OS, Hirsch T, Swami NS. Nanomaterialbased electrochemical sensing of neurological drugs and neurotransmitters. Microchimica Acta 2015; 182(1): 1-41.
- Singh JP, Thakur SN. Laser-Induced Breakdown Spectroscopy Elsevier 2007.
- Stavropoulos P, Palagas C, Angelopoulos GN, Papamantellos DN, Couris S. Calibration measurements in laser-induced breakdown spectroscopy using nanosecond and picosecond lasers. Spectrochimica Acta Part B: Atomic Spectroscopy 2004; 59(12): 1885-1892.
- Unnikrishnan VK, Alti K, Kartha VB, Santhosh C, Gupta GP, Suri BM. Measurements of plasma temperature and electron density in laser-induced copper plasma by time-resolved spectroscopy of neutral atom and ion emissions. Pramana 2010; 74(6): 983-993.
- Zhang Y, Yuan X, Wang Y, Chen Y. One-pot photochemical synthesis of graphene composites uniformly deposited with silver nanoparticles and their high catalytic activity towards the reduction of 2-nitroaniline. Journal of Materials Chemistry 2012; 22(15): 7245-7251.
- Al-Sawaff ZH, Rashid ZM, Yahya YZ, Kandemirli F. Electromagnetic field smart splint for bone fixing and rehabitation using niti shape memory alloy. NeuroQuantology 2020; 18(3): 37-44